Competing impurities and reentrant magnetism in $La_{2-x}Sr_xCu_{1-z}Zn_zO_4$: Role of Dzyaloshinskii-Moriya and *XY* anisotropies

L. Adamska,[1] M. B. Silva Neto,[2] and C. Morais Smith[1]
[1]*Institute for Theoretical Physics, University of Utrecht, Leuvenlaan 4, 3584 CE Utrecht, The Netherlands*
[2]*Institut für Theoretische Physik, Universität Stuttgart, Pfaffenwaldring 57, 70550, Stuttgart, Germany*
(Received 4 October 2006; revised manuscript received 31 January 2007; published 9 April 2007)

We study the order-from-disorder transition and reentrant magnetism in $La_{2-x}Sr_xCu_{1-z}Zn_zO_4$ within the framework of a long-wavelength nonlinear sigma model that properly incorporates the Dzyaloshinskii-Moriya and *XY* anisotropies. Doping with nonmagnetic impurities, such as Zn, is considered according to classical percolation theory, whereas the effect of Sr, which introduces charge carriers into the CuO_2 planes, is described as a dipolar frustration of the antiferromagnetic order. We calculate several magnetic, thermodynamic, and spectral properties of the system, such as the antiferromagnetic order parameter, σ_0, the Néel temperature, T_N, the spin-stiffness, ρ_s, and the anisotropy gaps, Δ_{DM} and Δ_{XY}, as well as their evolution with both Zn and Sr doping. We explain the nonmonotonic and reentrant behavior experimentally observed for $T_N(x,z)$ by Hücker *et al.*, [Phys. Rev. B **59**, R725 (1999)], as resulting from the reduction, due to the nonmagnetic impurities, of the dipolar frustration induced by the charge carriers (order-from-disorder). Furthermore, we find a similar nonmonotonic and reentrant behavior for all the other observables studied. Most remarkably, our results show that while for $x \approx 2\%$ and $z=0$ the Dzyaloshinskii-Moriya gap $\Delta_{\mathrm{DM}}=0$, for $z=15\%$ it is approximately $\Delta_{\mathrm{DM}} \approx 7.5\ \mathrm{cm}^{-1}$, and we expect it could be observed with one-magnon Raman spectroscopy.

DOI: 10.1103/PhysRevB.75.134507 PACS number(s): 74.25.Ha

I. INTRODUCTION

High temperature superconductivity is obtained by introducing charge carriers (holes or electrons) into Cu-based Mott-Hubbard insulators. At half-filling such systems exhibit long range antiferromagnetic (AF) order in the ground state, which is however rapidly suppressed by the introduction of charge carriers. Consider, for example, the case of La_2CuO_4, the simplest of the parent compounds. The replacement of La^{3+} by Sr^{2+} ions in $La_{2-x}Sr_xCuO_4$, through which holes are doped into the CuO_2 planes, causes the destruction of the canted Néel order already at $x \approx 0.02$,[1] showing that the doped holes strongly frustrate the underlying AF order within the CuO_2 planes. Conversely, doping of isovalent nonmagnetic impurities into La_2CuO_4 is known to have less dramatic effects. For example, by replacing Cu^{2+} for Zn^{2+} in $La_2Cu_{1-z}Zn_zO_4$,[2] the AF order is suppressed at much higher impurity concentration and the monotonic and rather smooth decrease of the Néel temperature T_N with z can be described, at least in the limit of low dilution, within classical percolation theory.

The combined effect of adding holes *and* nonmagnetic impurities into $La_{2-x}Sr_xCu_{1-z}Zn_zO_4$ was studied experimentally by Hücker *et al.*[3] It has been found that, even though each kind of impurity independently suppresses the AF order, an enhancement of the antiferromagnetism can occur when these impurities are combined. For example, in the presence of Zn, $z>0$, the AF order survives for $x>0.02$.[3] More interestingly, it was also found that for $x=0.017$, the Néel temperature exhibits a nonmonotonic behavior as a function of Zn doping. In fact, T_N is first enhanced from 125 K at $z=0$ to 144 K at $z=0.05$, and only then starts to be suppressed by the dilution (see Fig. 4 of Ref. 3).

This remarkable reentrant effect was immediately addressed theoretically by Korenblit *et al.*,[4] who first suggested that Zn reduces the frustration induced by Sr, through the dilution of ferromagnetic bonds. These authors started from the *two-dimensional and isotropic Heisenberg spin system* and obtained a phenomenological expression for the Néel temperature with the aid of a parameter α containing information about the Dzyaloshinskii-Moriya (DM) and pseudo-dipolar (*XY*) anisotropies, as well as the interplanar superexchange $J_\perp$. More recently, the same authors suggested that $J_\perp$ has little or nothing to do with the suppression of the AF order in $La_{2-x}Sr_xCu_{1-z}Zn_zO_4$ ($J_\perp$ was shown to be almost x and z independent), which should be, instead, solely determined by *intraplanar* correlations.[5] This is in agreement with the recent findings of Juricic *et al.*,[6] where it has been shown that the robustness of the canted Néel state is determined by the DM gap. The collinear long range AF order is destroyed when the renormalized DM gap vanishes, at $x \approx \Delta_{\mathrm{DM}}/J \sim 0.02$, and for higher doping the magnetism becomes incommensurate.[6,7] The DM and *XY* anisotropies have also been shown to be behind the unusual magnetic susceptibility response in $La_{2-x}Sr_xCuO_4$,[8,9] for a rather wide range in doping and temperature. In addition they are also responsible for the appearance of a field-induced mode in the one-magnon Raman spectrum of $La_{2-x}Sr_xCuO_4$.[10,11] Thus it is clear that any realistic description of the reentrant magnetism in $La_{2-x}Sr_xCu_{1-z}Zn_zO_4$ must properly take into account such anisotropies.

In this paper we revisit the problem of the reduction of frustration in $La_{2-x}Sr_xCu_{1-z}Zn_zO_4$, first proposed by Korenblit *et al.*,[4] within the framework of a long-wavelength nonlinear sigma model (NLSM) that properly includes DM and *XY* anisotropies, dilution, and frustration. We show that indeed dilution weakens the frustration by reducing the dipolar-magnon coupling constant. The result is a nonmonotonic behavior not only for T_N, but also for other observables like: order parameter, weak-ferromagnetic moment, and an-

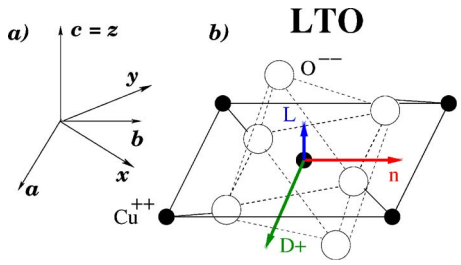

FIG. 1. (Color online) Left: Tetragonal (xyz) and orthorhombic (abc) coordinate systems. Right: In the LTO phase the tilting axis of the CuO_6 octahedra, represented by the vector $\mathbf{D}_+$ (in green), determines the orthorhombic a axis. The DM and XY anisotropies then determine that the staggered order parameter $\mathbf{n}$ (in red) is oriented along the orthorhombic b direction while the weak-ferromagnetic moment $\mathbf{L}$ (in blue) is perpendicular to the CuO_2 plane.

isotropy gaps. Moreover, since the destruction of the AF order is directly related to the vanishing of the DM gap,[6] we find that the reentrant antiferromagnetism is accompanied by a reentrant behavior for the DM gap itself. Finally, we show that the NLSM formulation, together with classical percolation theory, can also describe the experiments in the highly Zn-diluted limit, provided the appropriate bond percolation factor is used.

The paper is organized as follows. In Sec. II we discuss the different impurities to be considered, we review the derivation of the anisotropic NLSM for La_2CuO_4, introduce dilution by Zn according to the classical percolation theory, and include the dipolar frustration within the framework of the Shraiman and Siggia model.[12] In Sec. III we present our general model and compute all the renormalizations of the physical quantities. In Sec. IV we discuss the effect of the reduction of frustration in different physical quantities and propose experiments that could lead to the observation of these effects. This section is written in such a way that the reader not interested in the theoretical details can skip Secs. II and III. In Sec. V we present our conclusions. In Appendix A we review the continuum limit for the site and bond percolation factors, while in Appendix B we provide a detailed derivation of the NLSM with dilution.

II. IMPURITIES IN HOST La_2CuO_4

La_2CuO_4 is a layered antiferromagnet with a rather large XY anisotropy which below 530 K is in the low-temperature orthorhombic (LTO) phase. Although the orthorhombicity resulting from the staggered tilting of the CuO_6 octahedra is small, it is responsible for the presence of an antisymmetric exchange of the DM type once the spin-orbit coupling is considered. Together, these two anisotropies, DM and XY, gap the transverse spin-wave excitations along the a and c orthorhombic axis, respectively, and lead to a canted antiferromagnetic ordering along the b orthorhombic direction, see Fig. 1(b).

Theoretical studies of La_2CuO_4 concentrate on the Cu lattice, because all the other atoms (La^{3+}, O^{2-}) are in a closed shell configuration. In the crystal Cu^{2+} has a missing electron in the $d_{x^2-y^2}$ orbital, which carries a spin-$\frac{1}{2}$ and orders antiferromagnetically below $T_N=325$ K. There are two kinds of impurities which, at some value of doping, destroy the antiferromagnetic order in the layered La_2CuO_4 compound. Replacing La^{3+} with Sr^{2+} leads to a rapid suppression of the antiferromagnetic order in the plane. This happens because the holes donated to the planes form Zhang-Rice singlets with the local moments of Cu^{2+},[13] which act as effective mobile holes in the spin lattice. Doping the crystal with Zn, i.e., substituting Cu^{2+} with isovalent Zn^{2+}, introduces *vacancies* at the Cu positions. In fact, Cu^{2+} has an electronic configuration $[Ar]3d$,[9] while Zn^{2+} is $[Ar]3d$.[10] This means that there is no magnetic moment at the Zn position and therefore the effect of Zn doping is simply to dilute the spins within the plane.

The effect of the competition between Sr and Zn impurities in $La_{2-x}Sr_xCu_{1-z}Zn_zO_4$ was experimentally investigated in Ref. 3 and addressed theoretically in Refs. 4 and 14. Both theoretical works have, as a starting point, an isotropic quantum Heisenberg Hamiltonian on a square lattice. However, recent experimental[8,10,15] and theoretical[9,11,16–18] studies have emphasized the very important role of DM and XY anisotropies and thus we shall now describe the effect of dilution and frustration in an effective model including anisotropies.

A. Undoped La_2CuO_4

At long wavelengths, the isotropic Heisenberg Hamiltonian is well described, in the paramagnetic phase, by a $O(3)$ NLSM.[19] In this paper, however, we use a generalized NLSM, derived by Chovan and Papanicolaou in Ref. 16 and Silva Neto *et al.* in Ref. 9, which includes the DM and XY anisotropies. The action of the model reads

$$\begin{aligned} S_{\text{tot}} &= \int d\tau (L_H + L_{\text{DM}} + L_{XY} + L_{\text{WZ}}), \\ &= S^2 \sum_{\langle i,j \rangle} J \mathbf{\Omega}_i \mathbf{\Omega}_j + \mathbf{D}_{ij} \cdot (\mathbf{\Omega}_i \times \mathbf{\Omega}_j) + \mathbf{\Omega}_i \hat{\Gamma}_{ij} \mathbf{\Omega}_j \\ &\quad - iS \sum_{j \in 2D\text{lattice}} \delta \mathbf{\Omega}_j \cdot (\mathbf{\Omega}_j \times \partial_0 \mathbf{\Omega}_j). \end{aligned} \tag{1}$$

In Eq. (1), L_H, L_{DM}, L_{XY}, and L_{WZ} are, respectively, the Heisenberg, DM, XY, and Wess-Zumino terms, $\mathbf{\Omega}$ is a unit vector along the spin direction, $\mathbf{S}=S\mathbf{\Omega}$, and $S=1/2$. The super-exchange parameter is denoted by J. The DM vector $\mathbf{D}_{ij}$ and the anisotropy matrix $\hat{\Gamma}_{ij}$ are defined on the Cu-Cu bonds.[20,21] In the (x,y) coordinate system, see Fig. 1, $\mathbf{D}_x=(0,d,0)$, $\mathbf{D}_y=(d,0,0)$, $\hat{\Gamma}_x=\text{diag}(\Gamma_1+\Gamma_2,\Gamma_1-\Gamma_2,\Gamma_3)$, and $\hat{\Gamma}_y=\text{diag}(\Gamma_1-\Gamma_2,\Gamma_1+\Gamma_2,\Gamma_3)$. Here, the index x means along the horizontal Cu-O-Cu bonds, y means along the vertical Cu-O-Cu bonds, $d\sim 10^{-2}$ J, $\Gamma_{1,2,3}\sim 10^{-4}$ J, and $\Gamma_1>\Gamma_3$.

Our next step is to separate the fast $\mathbf{l}$ and slow $\mathbf{n}$ varying spin components,

$$\mathbf{\Omega}_i = (-1)^i \mathbf{n}_i \sqrt{1-(a\mathbf{l}_i)^2} + a\mathbf{l}_i \simeq (-1)^i \mathbf{n}_i + a\mathbf{l}_i - \frac{(-1)^i}{2} a^2 \mathbf{n}_i \mathbf{l}_i^2. \tag{2}$$

In Eq. (2) a is the lattice constant and i is an index on the 2D lattice, $i=(p,q)$; $(-1)^i$ should be understood as $(-1)^{p+q}$, $\mathbf{n}_i$ as

$\mathbf{n}_{p,q}$. After substituting Eq. (2) into Eq. (1) we find

$$S_{\rm tot} = \int d^2\mathbf{r}\left(\frac{JS^2}{2}[(\nabla\mathbf{n})^2 + 8\mathbf{l}^2] + \frac{4S^2}{a}\mathbf{d}_+\cdot(\mathbf{n}\times\mathbf{l}) + \frac{2S^2}{a^2}(\Gamma_1-\Gamma_3)n_z^2 - \frac{iS}{a}\mathbf{l}\cdot(\mathbf{n}\times\dot{\mathbf{n}})\right), \quad (3)$$

where $\mathbf{d}_+=(\mathbf{D}_x+\mathbf{D}_y)/2$.

B. Effect of nonmagnetic impurities—Zn doping

Recently, an effective field theory for the Heisenberg antiferromagnet with nonmagnetic impurities was derived by Chen and Castro Neto.[22] While in Ref. 22 the authors only considered the *isotropic* case, here we generalize the results of Ref. 22 to include the DM and *XY* anisotropies.

We introduce a function p_i, which is 1 on a Cu site and zero on a Zn site, with the property $p_i^2=p_i$. We then assume this function to be smooth and expand p_j in the neighborhood of its nearest neighbor site. In a continuum limit, p_i and $K_{ij}=p_ip_j$ are replaced, respectively, by $p(\mathbf{r})$ and $K(\mathbf{r})$, which are the so-called site and bond percolation factors. As it is shown in Appendix A, for the case of a homogeneous distribution of static impurities, they can be replaced by their average values, $P_\infty(z)=1-z$ and $K(z)=1-3z$. In the following we omit the z dependence in P_∞ and K for the sake of shortening the notation.

In the presence of dilution, the action (1) will be modified as follows: the terms L_H, $L_{\rm DM}$, and L_{XY}, which contain $\Sigma_{\langle i,j\rangle}f(\mathbf{\Omega}_i,\mathbf{\Omega}_j)$, will be multiplied by K. The Wess-Zumino term, on the other hand, contains $\mathbf{\Omega}_i^3$ and therefore it is proportional to $p^3(\mathbf{r})=p(\mathbf{r})$. Thus, within the homogeneous distribution assumption, it will be multiplied by P_∞. In this way, K and P_∞ appear simply as prefactors of the relevant integrals.[22] A detailed derivation of the NLSM in the presence of nonmagnetic impurities is given in Appendix B.

The next step is to integrate out $\mathbf{l}$ in Eq. (3) to obtain the action in the presence of dilution (see Appendix B)

$$S_{\rm Zn} = \frac{1}{2gc(K/P_\infty)}\int d\tau\int d^2\mathbf{r}\{(\partial_\tau\mathbf{n})^2 + Z[c^2(\nabla\mathbf{n})^2 + m_a^2n_a^2 + m_c^2n_c^2]\}, \quad (4)$$

where we have defined

$$Z = \frac{K^2}{P_\infty}, \quad (5)$$

g is the usual NLSM coupling constant, and c is the spin-wave velocity. Here we used that $\sqrt{2gcS^2/Ja^2}\mathbf{d}_+=2\sqrt{2}S\vec{de}_a=m_a\vec{e}_a$ and $(4gcS^2/a^2)(\Gamma_1-\Gamma_3)=32JS^2(\Gamma_1-\Gamma_3)=m_c^2$, where $\vec{e}_a$ is the unit vector along the a orthorhombic direction. Therefore, the last two terms in Eq. (4) correspond, respectively, to the DM and *XY* anisotropy gaps, showing that the spin ordering has an easy axis along the orthorhombic b direction, see Fig. 1.

From the above action it is clear that when only Zn impurities are doped into $La_2Cu_{1-z}Zn_zO_4$ the two anisotropy gaps renormalize according to

$$M_{a,c} = \sqrt{Z}m_{a,c}, \quad (6)$$

and thus decrease rather smoothly with dilution and vanish at the percolation threshold.

In what follows we shall switch freely between $\Delta_{\rm DM}$ and M_a, when referring to the DM or in-plane gap, and also between Δ_{XY} and M_c, when referring to the *XY* or out-of-plane gap, without any loss of generality.

C. Derivation of the Néel temperature

Let us now derive an expression for the Néel temperature in terms of the anisotropy gaps and spin stiffness. Our approach follows closely previous studies of the Néel temperature in easy axis[23] and easy-plane[24] antiferromagnets, but now we consider also renormalization due to dilution. Starting from the action in Eq. (4), we split the $\mathbf{n}$-field into its longitudinal σ_0 and transverse $\mathbf{n}_\perp$ components, $\mathbf{n}=(n_a,\sigma_0,n_c)$. Here $\mathbf{n}_\perp=(n_a,n_c)$, and $\sigma_0=$const is the order parameter. The action then reads

$$S^d[\mathbf{n}_\perp] = \frac{1}{2gc}\frac{1}{\beta}\sum_{\omega_n}\int\frac{d^2\mathbf{k}}{(2\pi)^2}\mathbf{n}_\perp\hat{A}^d\mathbf{n}_\perp, \quad (7)$$

with

$$\hat{A}^d = \mathbf{I}_2[(P_\infty/K)\omega_n^2 + Kc^2\mathbf{k}^2] + {\rm diag}[Km_a^2, Km_c^2], \quad (8)$$

where $\omega_n=2\pi n/\beta$ are the Matsubara frequencies, $\mathbf{I}_2$ is a 2D identity matrix, and $\beta=1/k_BT$ is the inverse temperature. Defining Tr as $\beta^{-1}\Sigma_{\omega_n}\int d^2\mathbf{k}/(2\pi)^2$ and introducing the fixed length constraint into the action through a Lagrange multiplier, λ, the partition function can be written as

$$\begin{aligned} Z &= \int D\mathbf{n}\,\delta(\mathbf{n}^2-P_\infty)\exp\{-S^d[\mathbf{n}]\} \\ &= \int D\sigma_0 D\mathbf{n}_\perp D\lambda\,\exp\left(-\frac{1}{2gc}\right. \\ &\quad \left.\times{\rm Tr}[\mathbf{n}_\perp\hat{A}^d\mathbf{n}_\perp + i\lambda(\sigma_0^2+\mathbf{n}_\perp^2-P_\infty)]\right) \\ &= \int D\sigma_0 D\lambda\,\exp\{-S_{\rm eff}[\lambda,\sigma_0]\}, \end{aligned} \quad (9)$$

where the effective action reads

$$S_{\rm eff}[\lambda,\sigma_0] = \frac{1}{2gc}{\rm Tr}[i\lambda\sigma_0^2 - i\lambda P_\infty] + \frac{1}{2}\sum_{\alpha=a,c}{\rm Tr}\,\ln[A^d_{\alpha\alpha}+i\lambda]. \quad (10)$$

In Eqs. (9) and (10) we used the average length of spin per lattice site P_∞ in the diluted case.[22,25]

The thermodynamic properties of the diluted system can be determined, at the mean field level, by solving the saddle point equations of the effective action (10). From $\delta S_{\rm eff}[\lambda,\sigma_0]/\delta\lambda=0$ we find

$$\frac{P_\infty - \sigma_0^2}{gc} = \sum_{\alpha=a,c} \mathrm{Tr} \frac{1}{A^d_{\alpha\alpha} + i\lambda}. \quad (11)$$

The only condition for the trace to converge is to choose $i\lambda = m_0^2$, a real positive number. As usual, we interpret it as the inverse correlation length, $m_0 = 1/\xi$.

At the Néel critical point the order parameter σ_0 vanishes, the correlation length ξ diverges, and the equation for the critical temperature is

$$\frac{\beta P_\infty^2}{gcK} = \sum_{\alpha=a,c} \sum_{\omega_n} \int \frac{d^2\mathbf{k}}{(2\pi)^2} \frac{1}{\omega_n^2 + Zc^2(\mathbf{k}^2 + m_\alpha^2/c^2)}.$$

After performing the Matsubara summation and the integration over momenta, the last expression simplifies to

$$4\pi\beta_N P_\infty K\rho_s + \sum_{\alpha=a,c} \ln\left[2\sinh\left(\frac{\beta_N}{2}\sqrt{Z}m_\alpha\right)\right] = 0, \quad (12)$$

where $\beta_N = 1/k_B T_N$ and we defined the renormalized spin stiffness for the diluted system

$$\rho_s = c\left(\frac{1}{2g} - \frac{1}{g_c K P_\infty}\right), \quad (13)$$

with g_c defined through the ultraviolet momentum cutoff $\Lambda = 4\pi/g_c$, as usual.

The bond percolation factor $K(z) = 1 - 3z$, proposed in Ref. 22, (see Appendix A) describes well the experimental data for $T_N(z)$ only in the low doping range.[3,22] For highly diluted samples, however, single crystals were not available before the work reported in Ref. 2. The experiments were usually performed with single crystal samples below the doping threshold of $z \approx 20\%$, while above 25% powder samples were used. After Ref. 2, which used both single crystals and powder samples, our conclusion is that for the heavily doped samples the bond percolation factor should be modified according to Refs. 26 and 27, which suggest that $K(z) = 1 - \pi z + \pi z^2/2$. In this Watson-Leath (WL) prescription, T_N is zero at the percolation threshold, z_p. Theoretical, experimental, and numerical studies of highly diluted $La_2Cu_{1-z}[Mn,Zn]_zO_4$ are presented in Ref. 2. There the authors describe an experiment where the critical point is found at $z = 42\%$. As it is observed in Fig. 2, using the bond percolation factor as in the WL prescription, we obtain the correct description in the heavily doped regime.

It should be remarked at this point that the quantum Monte Carlo simulations by Sandvik[28] can also correctly describe the behavior of the staggered order parameter and two-dimensional (2D) correlation length, as a function of dilution, within the framework of a bilayer square-lattice Heisenberg model. Here, instead, we consider only a single CuO_2 layer, but we include the DM and *XY* anisotropies which are enough to stabilize the long range Néel order at finite temperature. The importance of the DM and *XY* anisotropies can be understood from the recent results by Korenblit *et al.*,[5] who demonstrated that $J_\perp$ has little to do with the suppression of the AF order in Sr and Zn doped $La_{2-x}Sr_xCu_{1-z}Zn_zO_4$, which should be, instead, completely determined by *intraplanar* correlations.

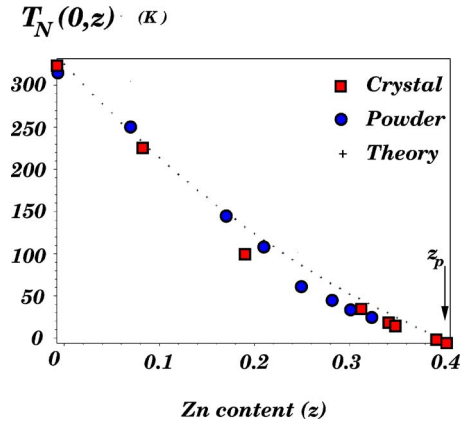

FIG. 2. (Color online) Néel temperature (in K) as a function of Zn concentration for $x=0$ up to the highly diluted regime. The experimental data for either powder and crystal samples was taken from Refs. 2 and 3.

For the plot in Fig. 2 we used $J = 100$ meV, which is much smaller than the real value of ≈ 135 meV, but is the value that gives $T_N(x=0, z=0) = 325$ K within our saddle-point approximation. The inclusion of fluctuations away from the saddle point can allow for the more realistic value of J to be used. In the next section we discuss the effect of Sr doping and in the following we shall concentrate our studies on single crystals doped simultaneously with Sr and Zn.

D. Effect of frustration—Sr doping

In order to incorporate the effect of Sr doping in $La_2Cu_{1-z}Zn_zO_4$, we adopt the Shraiman and Siggia model.[12] In this model the holes introduced in the system $(La_{2-x}Sr_xCu_{1-z}Zn_zO_4)$ via Sr doping are represented by an effective dipolar field that couples to the background magnetization current.[12] In Ref. 6 it was shown that this interaction leads to a reduction of the magnon gaps and spin stiffness, in agreement with the experiments.[10] As we shall now demonstrate, such reduction is not as strong if the compound is additionally doped with Zn, since in the presence of nonmagnetic impurities the effective dipole-magnetization-current interaction should be multiplied by the bond dilution factor. This mechanism of reduction of frustration by nonmagnetic impurities has been considered earlier by Korenblit *et al.*[4] within the isotropic $O(3)$ NLSM. Here we discuss the role of anisotropies.

In the Shraiman-Siggia model the interaction between magnons and the dipolar field *in the absence of dilution* can be written as

$$S_{\mathrm{int}} = -2\lambda \int d\tau \int d^2\mathbf{r} \mathbf{P}_\mu \cdot \mathbf{n} \times \partial_\mu \mathbf{n}, \quad (14)$$

where

$$\mathbf{P}_\mu = i\partial_\mu \bar{\Psi} \vec{\sigma} \Psi + \mathrm{H.c.}, \quad (15)$$

$\mathbf{P}_\mu$ is the dipolar field representing the spin current of the holes, Ψ is the spinor wave function of the doped holes with dispersion centered at $(\pi/2, \pm\pi/2)$ and symmetry related

points in the Brillouin zone, $\vec{\sigma}$ are the three Pauli matrices, and μ is a lattice index. The origin of such dipolar field is simple. As the doped holes hop, they produce a transverse dipolar distortion (a twist) in the staggered order parameter field, as described by Eq. (14). Such twist occurs in order to minimize the hole's kinetic energy and originates from the coupling of two spin currents: the hole's spin current (here represented by the dipolar field $\mathbf{P}_\mu$) and the magnetization current $\mathbf{J}_\mu = \mathbf{n} \times \partial_\mu \mathbf{n}$.[12]

In the presence of dilution the above dipole-magnon interaction will also have to be modified following the procedure described in Appendix B. Essentially, one can represent the semiclassical background spin distortion as a slowly varying SU(2) rotation of the Néel state $\mathbf{R}_\mathbf{r}$. The hopping term for the doped holes involves the product $\mathbf{R}_r \mathbf{R}^+_{r+\mathbf{a}}$, and since these are rotations in neighboring sites, i.e., $\mathbf{R}_i \mathbf{R}^+_j$, in the presence of dilution this product must be replaced by

$$\mathbf{R}_i \mathbf{R}^+_j \rightarrow \mathbf{R}_i \mathbf{R}^+_j p_i p_j, \tag{16}$$

where i, j are nearest neighbor sites. Consequently, the coupling constant λ between the dipolar field and the background magnetization current in Eq. (14) should be changed according to

$$\lambda \rightarrow K\lambda, \tag{17}$$

because (14) comes from (16).[12] Here K is the bond dilution factor which in the homogeneous approximation is given by $K = \langle p_i p_j \rangle$.

III. GENERAL MODEL

The complete action describing the simultaneous effect of magnetic dilution by Zn and frustration by Sr reads

$$S = \frac{1}{2gc(K/P_\infty)} \int d\tau \int d^2\mathbf{r} \{ (\partial_\tau \mathbf{n})^2 + Z[c^2(\nabla \mathbf{n})^2 + m_a^2 n_a^2 + m_c^2 n_c^2] \} - 2\lambda K \int d\tau \int d^2\mathbf{r} \, (\mathbf{P}_\mu \cdot \mathbf{n} \times \partial_\mu \mathbf{n}) + S_d, \tag{18}$$

where

$$S_d = \frac{1}{2} \int d\tau \int d^2\mathbf{r} \mathbf{P}_\mu G_D^{-1} \mathbf{P}_\mu \tag{19}$$

describes the fluctuations of the dipolar field. Since the dipolar field is a pseudo-fermionic composite field, it is an operator that represents the spin current of the doped holes, the dipolar susceptibility (inverse dipole propagator) can be obtained from a polarization diagram (see Fig. 3).

In what follows we adopt the same procedure used by Sachdev in Ref. 29 and we use the results from the Fermi liquid polarization diagram in two dimensions. However, while in Ref. 29 the ballistic limit (clean system) was used in the calculation of the polarization diagram, see the left-hand diagram in Fig. 3, here we consider the diffusive limit (dirty system) because of the scattering of the doped holes by the Sr impurities, see middle diagram in Fig. 3. This assumption

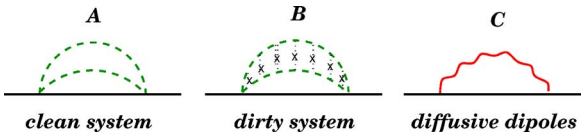

FIG. 3. (Color online) Contribution to the magnon propagator from the dipolar fields. The figure on the left (A) contains the polarization diagram of the doped holes. In (B) we introduce disorder through the scattering of the holes by impurities and this is represented effectively by the magnon-dipole bubble diagram (C) where we use the diffusive dipole propagator.

is consistent with recent results from Lüscher *et al.*[18] who have shown that the dynamics of these dipolar fields is highly diffusive. Thus, we shall write for the dipole propagator in the diffusive limit (see the right-hand diagram in Fig. 3)

$$G_D(\mathbf{q}, \omega_n) = \kappa_d \frac{D\mathbf{q}^2}{D\mathbf{q}^2 + |\omega_n|}, \tag{20}$$

where κ_d is proportional to the inverse static susceptibility and D is the diffusion constant, which is assumed to be large.

Because of the peculiar dipolar-magnon coupling from Eq. (14), the magnon propagator will be renormalized by the fluctuations of the dipolar field (see Fig. 3). The self-energy correction to the magnon propagator is

$$\Sigma^\alpha_M(\mathbf{q}, \omega_n) = \kappa_d(\lambda^2 K^2) \frac{gcK}{P_\infty} \times \sum_{\beta \neq \alpha} \frac{1}{\beta} \sum_{\omega_n} \frac{d^2\mathbf{k}}{(2\pi)^2} \frac{(\mathbf{k}+2\mathbf{q})^2}{\omega_n^2 + Zc^2(\mathbf{k}+\mathbf{q})^2 + Zm_\beta^2} \frac{D\mathbf{k}^2}{D\mathbf{k}^2 + |\omega_n|}. \tag{21}$$

By summing up the one-loop corrections to the magnon Green's function, we obtain

$$\widetilde{G}_M = G_M \sum_{i=0}^{\infty} (\Sigma_M G_M)^i = [G_M^{-1} - \Sigma_M]^{-1}. \tag{22}$$

Writing this expression explicitly, we get for the magnon propagator

$$\widetilde{G^\alpha_M}^{-1}(\mathbf{q}, \omega_n) = (gcK/P_\infty)^{-1}(\omega_n^2 + Zc^2\mathbf{q}^2 + Zm_\alpha^2) - \Sigma^\alpha_M(\mathbf{0}) - \frac{1}{2} q_\mu q_\nu \frac{\partial^2 \Sigma^\alpha(\mathbf{q})}{\partial q_\mu \partial_\nu}\bigg|_{\mathbf{q}=0}, \tag{23}$$

where we expanded the self-energy around zero momentum up to the second order term, in order to obtain a correction to the gaps and spin stiffness, and thus

$$\widetilde{G^\alpha_M}^{-1}(\mathbf{q}, \omega_n) = \left(\frac{gcK}{P_\infty}\right)^{-1} \omega_n^2 + \left[\frac{Kc}{g} - \frac{\delta_{\mu\nu}}{2} \frac{\partial^2 \Sigma^\alpha_M(\mathbf{q}, 0)}{\partial q_\mu \partial q_\nu}\bigg|_{\mathbf{q}=0}\right] \mathbf{q}^2 + \left(\frac{gcK}{P_\infty}\right)^{-1} \left[Zm_\alpha^2 - \frac{gcK}{P_\infty} \Sigma^\alpha(0,0)\right]. \tag{24}$$

From the above equation the expressions for the mass and the spin stiffness renormalizations are readily derived

$$M_\alpha^2(x,z) = Zm_\alpha^2 - \frac{gcK}{P_\infty}\Sigma^\alpha(0,0) \quad \text{and}$$

$$\rho_s(x,z) = K\rho_s - \sum_{\alpha=a,c} \frac{\delta_{\mu\nu}}{2} \frac{\partial^2 \Sigma_M^\alpha(\mathbf{q},0)}{\partial q_\mu \partial q_\nu}\bigg|_{\mathbf{q}=0}, \tag{25}$$

where $\rho_s = c/2g$ is the bare spin stiffness in a clean system. Explicitly, the mass renormalization due to Sr and Zn impurities reads

$$M_\alpha^2(x,z) = Z[m_\alpha^2 - \kappa_d(gc\lambda)^2 Z I^\alpha(z)], \tag{26}$$

where

$$I^\alpha(z) = \sum_{\beta\neq\alpha} \frac{1}{\beta} \sum_{\omega_n} \int \frac{d^2\mathbf{k}}{(2\pi)^2} \frac{\mathbf{k}^2}{\omega_n^2 + Zc^2\mathbf{k}^2 + Zm_\beta^2} \frac{D\mathbf{k}^2}{D\mathbf{k}^2 + |\omega_n|}. \tag{27}$$

The spin stiffness, on the other hand, renormalizes according to the formula

$$\rho_s(x,z) = K\rho_s \Bigg[1 - \sum_{\beta=a,c} \frac{1}{2\beta} \sum_{\omega_n} \int \frac{d^2\mathbf{k}}{(2\pi)^2} \times \Bigg(\frac{\partial^2}{\partial \mathbf{q}^2} \frac{(\mathbf{k}+2\mathbf{q})^2}{\omega_n^2 + Zc^2(\mathbf{k}+\mathbf{q})^2 + Zm_\beta^2}\bigg|_{\mathbf{q}=0} \Bigg) \times \frac{D\mathbf{k}^2}{D\mathbf{k}^2 + |\omega_n|} \Bigg]. \tag{28}$$

The new momentum cutoff Λ for the dipoles, which renormalizes the spin stiffness, is set by $k_F = \sqrt{\pi x}$, because our theory should be valid at distances much larger than the average distance between the Sr impurities.

In the zero temperature, $T \to 0$, and highly diffusive, $D \to \infty$, limits the expressions for M_α and ρ_s read

$$M_\alpha^2[x,z;T\to 0] = Z\Bigg(m_\alpha^2 - \kappa_d(gc\lambda)^2 \sum_{\beta\neq\alpha} Z^{1/2} \frac{m_\beta^3}{4\pi c^4} \times \Bigg\{ \frac{1}{3}\Bigg[\Bigg(1 + \frac{k_F^2c^2}{m_\beta^2} \Bigg)^{3/2} - 1 \Bigg] - \Bigg[\Bigg(1 + \frac{k_F^2c^2}{m_\beta^2} \Bigg)^{1/2} - 1 \Bigg] \Bigg\} \Bigg), \tag{29}$$

and

$$\rho_s[x,z;T\to 0] = K\rho_s \Bigg[1 - \sum_{\beta=a,c} \frac{\kappa_d(gc\lambda)^2 Z^{1/2} m_\beta}{4\pi c^4} \times \Bigg(1 + \frac{\Big(\frac{k_F^2c^2}{m_\beta^2}\Big)^2 + \frac{1}{2}\frac{k_F^2c^2}{m_\beta^2} - 1}{\Big(1 + \frac{k_F^2c^2}{m_\beta^2}\Big)^{3/2}} \Bigg) \Bigg]. \tag{30}$$

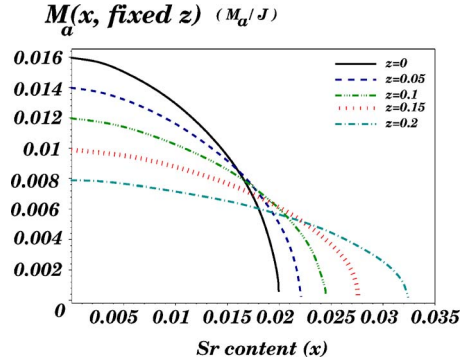

FIG. 4. (Color online) Dependence of the DM gap ($\Delta_{DM} = M_a$, in units of J) on Sr doping x at various fixed Zn concentration: $z = 0, 0.05, 0.1, 0.15, 0.2$. Although Zn and Sr independently reduce M_a, when combined an enhancement of M_a does occur.

IV. OBSERVABLES

Equations (29) and (30) are the most important results of this paper. As we can clearly see, although both M_α and ρ_s are reduced when only Sr ($\lambda \neq 0$ and $Z=1$) or only Zn ($\lambda = 0$ and $Z<1$) are doped *independently* into La_2CuO_4, when combined a nonmonotonic and reentrant behavior can indeed occur due to the $\lambda^2\sqrt{Z}$ coefficient in the self-energy correction [see Eqs. (29) and (30)].

In what follows we discuss the evolution with both Zn and Sr doping of several spectral, thermodynamic, and magnetic properties of the $La_{2-x}Sr_xCu_{1-z}Zn_zO_4$ system using the results obtained from the preceding section. As we shall see, the nonmonotonic behavior of different physical observables, such as the order parameter, the Néel temperature, and the weak-ferromagnetic moment, all follow from the nonmonotonicity induced by the competition between dilution and frustration in M_α and ρ_s.

A. Dzyaloshinskii-Moriya or in-plane gap

Juricic *et al.*[6] have recently studied the evolution of the DM gap with Sr in $La_{2-x}Sr_xCuO_4$ (see also Lüscher *et al.*[18]). One of the most important findings reported in Ref. 6 was that the DM gap gives *robustness* to the canted Néel state and vanishes at a critical concentration given by $x=$const $(\Delta_{DM}/J) \approx 2\%$, where const is $O(1)$ (see also curves in Figs. 4 and 5). The mechanism for the reduction of the DM gap was traced back to the self-energy corrections due to the dipolar frustration introduced by Sr doping, M_α with $Z=1$ ($z=0$), and the theoretical curve was shown to agree quite well with the one-magnon Raman experiments of Gozar *et al.*[10]

In fact, these experiments, performed at 10 K, show that at $x=z=0$ the Dzyaloshinskii-Moriya (or in-plane) gap is $m_a = 17.5\ \text{cm}^{-1}$ (or 2.16 meV), whereas it is reduced by almost 30% at $x=1\%$, and it vanishes at $x=2\%$. In Fig. 4 we exhibit the Sr dependence of the DM gap for various fixed Zn concentrations (the DM gap is given in units of J). As it is evident from the plot, for small x and z the DM gap is always reduced. At large x, however, a reentrant behavior is observed already for very small Zn concentration. This increase

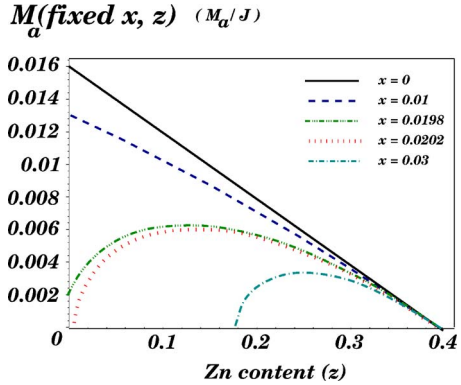

FIG. 5. (Color online) Dependence of the DM gap ($\Delta_{\mathrm{DM}}=M_a$, in units of J) on Zn doping z at various fixed Sr concentrations: $x=0$, 0.01, 0.0198, 0.0202, 0.03. The nonmonotonic and reentrant behaviors for M_a is evident.

of the DM gap is largest close to the Zn-free critical concentration $x=2\%$. In fact, while for $x=2\%$ and $z=0$ the DM gap is zero,[6,10] we find that for $x=2\%$ and $z=15\%$ the DM gap is $\Delta_{\mathrm{DM}}\approx 7.5\ \mathrm{cm}^{-1}$. Thus, we predict that low-energy Raman experiments in $La_{2-x}Sr_xCu_{1-z}Zn_zO_4$ samples with $x\approx 2\%$ and $z=15\%$ should observe a clear signal of a one-magnon mode with energy close to $7.5\ \mathrm{cm}^{-1}$ in the B_{1g} scattering geometry,[11,30] such as the ones performed by Gozar *et al.*[10] in Zn-free samples.

Figure 5 shows the evolution of the DM gap as a function of Zn doping for various fixed Sr concentrations. The nonmonotonic (for $x=0.0198$) and reentrant (for $x\geq 0.02$) behaviors predicted by our theory for the DM gap are also evident from this plot. As expected, all curves collapse into a single curve in the highly Zn-diluted regime. For completeness we show in Fig. 6 a three-dimensional (3D) plot with the evolution of the DM gap with both Zn and Sr doping.

As we have discussed in the preceding section, the key mechanism for such nonmonotonic and reentrant behavior observed in the DM gap, through dilution by Zn, is the *decrease* of the effective dipolar-magnon coupling constant $\lambda \rightarrow K\lambda$ in Eq. (17), which therefore reduces the self-energy corrections to the magnon gaps, see Eq. (29).

Let us now list a number of predictions from our studies, for a few selected doping concentrations of Sr and Zn, that can be verified experimentally.

(1) For $La_2Cu_{0.96}Zn_{0.04}O_4$, that is $x=0$ and $z=0.04$ where

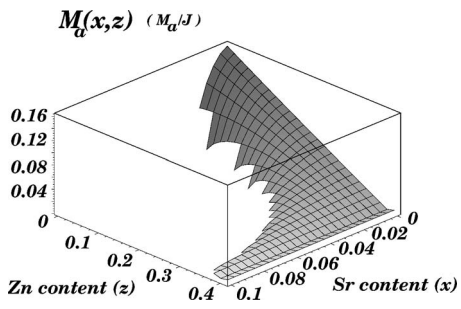

FIG. 6. 3D plot with the dependence of the DM gap ($\Delta_{\mathrm{DM}}=M_a$, in units of J) on both Sr and Zn doping.

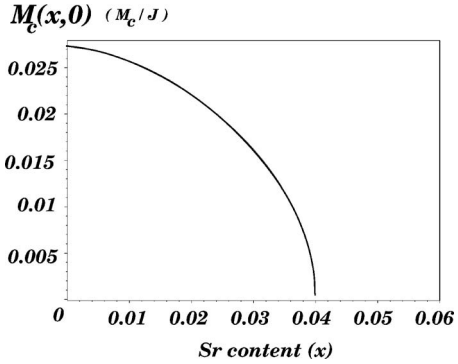

FIG. 7. Dependence of the XY gap ($\Delta_{XY}=M_c$, in units of J) on Sr doping x at zero Zn concentration, $z=0$.

$\sqrt{Z}\approx 0.9$, we estimate that the reduction of the DM gap will be of about 10% from the undoped $x=z=0$ value.

(2) For $La_{1.99}Sr_{0.01}Cu_{0.97}Zn_{0.03}O_4$, that is $x=0.01$ and $z=0.03$ where $\sqrt{Z}\approx 0.92$, the reduction of the DM gap will be smaller than the naive 36% expected from the 8% reduction, due to Zn, over the 30% reduction due to Sr. This is due to the dilution of frustration in the dipole-magnon coupling and we thus predict that the reduction will be of only 27% from the undoped $x=z=0$ value.

(3) For $La_{1.98}Sr_{0.02}Cu_{0.85}Zn_{0.15}O_4$, that is $x=0.02$ and $z=0.15$ where $\sqrt{Z}\approx 0.6$, we predict that the Dzyaloshinskii-Moriya gap is actually nonzero. In fact, due to the reduction of 40% in the dipole-magnon interaction, the DM gap is found to be $7.5\ \mathrm{cm}^{-1}$ and thus large enough, so that it can be accessed with one-magnon Raman spectroscopy.

B. *XY* or out-of-plane gap

The mechanism for the reduction of the XY gap is the same as the one discussed in the preceding section, see Eq. (29). For the XY gap the available data also comes from one-magnon Raman spectroscopy experiments.[10] For $x=z=0$ and at 10 K the XY gap is $m_c=36\ \mathrm{cm}^{-1}$ (or 4.3 meV), and is reduced by almost 15% at $x=1\%$.

The dependence of the XY gap on Sr doping, according to our theory, is shown in Fig. 7. We find that at $x=1\%$ and $z=0$ the XY gap is reduced by almost 10%, which is not far from the experimentally measured value, and it vanishes at $x=0.04$. When Zn is also included in the calculations we obtain a similar nonmonotonic and reentrant behavior, as observed for the DM gap (see the 3D plot in Fig. 8).

The vanishing of the XY gap at $x=4\%$ for $z=0$ has another very interesting consequence. As it has been proposed by Juricic *et al.*,[6] for $z=0$ and $x>0.02$, after the DM gap has disappeared, the magnetism becomes incommensurate (the staggered moment becomes helicoidal along the b axis) with an incommensurate wave vector $\mathbf{Q}\|b$ and with magnitude

$$Q=\sqrt{x^2-\tilde{M}_c(x,0)^2}, \tag{31}$$

where $\tilde{M}_c=M_c/J$ is dimensionless. As a consequence of the nonzero character of M_c, the incommensurability for $0.02<x<0.04$ deviates from the linear behavior $Q=x$, see Fig. 9,

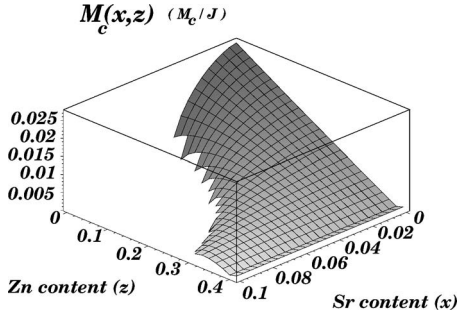

FIG. 8. 3D plot with the dependence of the XY gap ($\Delta_{XY}=M_c$, in units of J) on both Sr and Zn doping.

as indeed observed experimentally.[31] For higher Sr doping, however, when $M_c(x>0.04)=0$, the linear relation $Q=x$ becomes exact.[31]

When Zn is codoped into the Sr doped sample, for example, $20\%<z<40\%$ and $x=5\%$, the reentrant behavior for the XY gap, $M_c(x,z)>0$, depicted in Fig. 8, suggests that the incommensurability should decrease as the Zn concentration is increased [see Eq. (31)]. Such decrease of the incommensurability due to the enhancement of the magnetism through dilution of frustration has been predicted earlier by Hasselmann *et al.* in Ref. 32 and has been recently confirmed with neutron scattering by Matsuda *et al.* in Ref. 33.

C. Order parameter

Because of the DM and XY anisotropies, at zero applied magnetic field the staggered order parameter is oriented along the orthorhombic b axis with magnitude $\sigma_0(x,z)$. In the presence of a longitudinal magnetic field, $\mathbf{B}\|b$, the spins start to rotate on the bc plane as described theoretically by Silva Neto and Benfatto in Ref. 11 (see also Benfatto *et al.* in Ref. 30) and experimentally measured with neutron diffraction by Reehuis *et al.* in Ref. 15. At a critical field determined by the DM gap,

$$H_c(x,z)=M_a(x,z), \tag{32}$$

a spin-flop transition occurs, where the in-plane component of the order parameter becomes oriented along the orthorhombic a axis. Thus, any nonmonotonic and reentrant behavior of the DM gap will result on a similar reentrant behavior for the critical field. This is a prediction that could be detected by neutron scattering experiments.

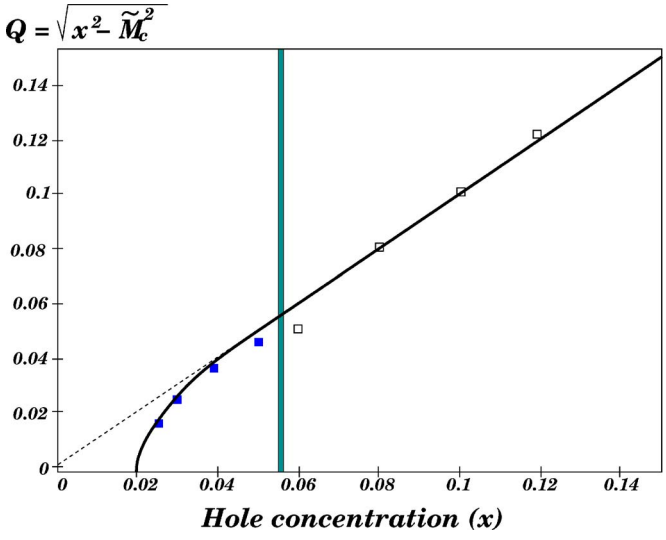

FIG. 9. (Color online) Plot of the incommensurability $Q=\sqrt{x^2-\tilde{M}_c^2}$ as a function of doping x. The dashed line is the $Q=x$ line. Notice that as the XY gap vanishes $M_c\to 0$, the IC peaks should approach the linear relation $Q=x$, as observed experimentally. The vertical line at $x\approx 0.055$ separates the insulating (left) and metallic (right) phases. The data points are from Ref. 31.

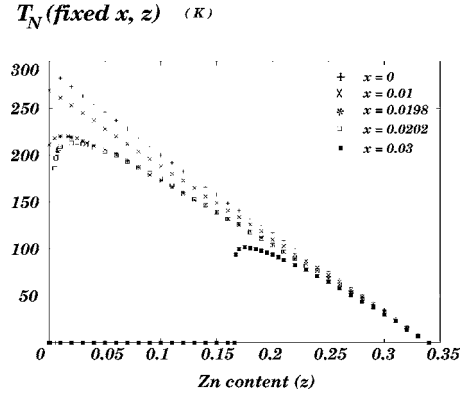

FIG. 10. Dependence of T_N (in K) on Zn doping z at various fixed Sr concentrations $x=0$, 0.01, 0.0198, 0.0202, 0.03. The nonmonotonic and reentrant behaviors are evident.

D. Néel temperature

In the case of single crystals doped with Sr and Zn, the available data from Ref. 3 were obtained with samples which contained less than 30% of Zn. Therefore, in this doping range the dependence of $T_N(z)$ is linear and is well described with the bond percolation factor $K(z)=1-3z$.

The Néel temperature, $T_N(x,z)$, where the order parameter vanishes, is given by Eq. (12), with the stiffness and magnon gaps renormalized by the impurities, see Eqs. (29) and (30). As it happens with the DM gap, we find that T_N exhibits a nonmonotonic and reentrant behavior as the Zn concentration is increased, see Fig. 10. In particular, we find a monotonic decrease in the slope of the curves $T_N(x,z=0)$ and $T_N(x,z=0.15)$, in qualitative agreement with the experiments of Hücker *et al.*,[3] see Fig. 11. Since we neglect the self-consistent renormalization of the magnon gaps with temperature, the agreement of our theoretical curves for T_N with experiments is only qualitative, in contrast to the low-temperature results for the DM gap discussed above, which are quantitative.

It is worth emphasizing that the nonmonotonic behavior exhibited by our theoretical curve $x=0.0198$ in Fig. 10 is experimentally observed already at $x=0.017$. Moreover, the 2D-Ising-like behavior of the curves in Fig. 11 are actually an artifact of the dimensionality (we are considering an easy-axis 2D NLSM) and of the approximation (we are neglecting the thermal renormalizations of the gaps). We expect that by

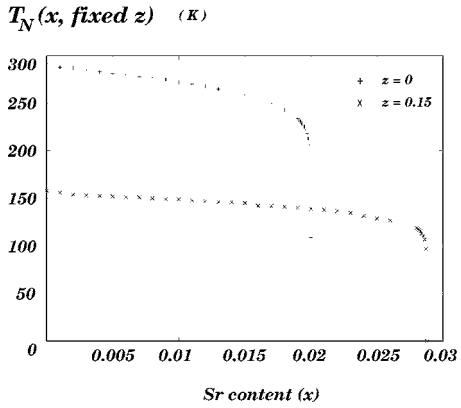

FIG. 11. Dependence of T_N (in K) on Sr doping x at two different Zn concentrations, $z=0$ and $z=0.15$. The slope of the curves decreases monotonically with increasing Zn content.

including the self-consistent thermal renormalizations and interlayer coupling, the agreement between theory and experiment in Fig. 11 will be satisfactory. Nevertheless, the qualitative agreement with experiments gives strong support to the model and mechanisms considered here.

E. The weak-ferromagnetic moment

The staggered pattern of tilted octahedra in La_2CuO_4 is known to be responsible for a weak-ferromagnetism, signaled by a cusp in the low-field magnetic susceptibility.[34] Within the language of the NLSM (see Ref. 9), such weak-ferromagnetic moment is proportional to the Néel order parameter via the equation

$$\langle \mathbf{L} \rangle = \frac{1}{2J}[\langle \mathbf{n} \rangle \times \mathbf{D}_+]. \tag{33}$$

Since within the Néel phase the average value of the staggered magnetization is $\langle \mathbf{n} \rangle = (0, \sigma_0, 0)$ (in the *abc* orthorhombic coordinate system), any nonmonotonic and reentrant behavior observed in σ_0 will cause also a similar effect in the weak-ferromagnetic moment, and this can be accessed in magnetic susceptibility experiments.

V. CONCLUSIONS AND OUTLOOK

In this paper we revisited the problem of the dilution of frustration in $La_{2-x}Sr_xCu_{1-z}Zn_zO_4$, within the framework of a generalized NLSM that includes DM and *XY* anisotropies. We showed that dilution by Zn weakens the frustration by Sr through the reduction of the dipole-magnon coupling constant, see Eq. (17). This leads to a nonmonotonic and reentrant behavior not only for T_N but also for other observables like the order parameter, the weak-ferromagnetic moment, and the anisotropy gaps.

Most remarkably, we predict that for $x \approx 2\%$ and $z = 15\%$ the DM gap is approximately 7.5 cm^{-1}, and thus likely to be observed in one-magnon Raman scattering. Furthermore, when the WL expression for the bond percolation factor is incorporated into our NLSM description, not only as a reduction factor for the spin stiffness but also and most importantly for the reduction of the anisotropy gaps, we find that our NLSM with dilution describes correctly the data for $T_N(x=0,z)$, also in the highly Zn-diluted regime. Finally, we have also found that the *XY* gap vanishes, in the absence of dilution, for $x=0.04$ and this is consistent with the deviation from linearity, for $0.02 < x < 0.04$, of the incommensurate peaks seen in neutron scattering within the spin-glass phase of $La_{2-x}Sr_xCuO_4$.

ACKNOWLEDGMENTS

The authors acknowledge useful discussions with A. Aharony, Yoichi Ando, L. Benfatto, G. Blumberg, A. Castro Neto, Yu-Chang Chen, A. Gozar, N. Hasselmann, and V. Juricic.

APPENDIX A: DERIVATION OF SITE AND BOND PERCOLATION FACTORS

This derivation can be found also in Ref. 25, but for the sake of completeness we will go through the basic steps of the derivation.

Averaging the site percolation factor we obtain

$$P_\infty = P_\infty(z) = \frac{1}{Na^2}\int d^2\mathbf{r} p(\mathbf{r}) = \frac{a^2(N - N_{\text{Zn}})}{Na^2}$$
$$= 1 - N_{\text{Zn}}/N = 1 - z, \tag{A1}$$

where averaging $p(\mathbf{r})$ over a 2D volume implies that we must normalize it with Na^2, N being the number of sites in the Cu lattice.

We consider p_j to be smooth, and thus we can expand it in the neighborhood of the ith site $p_j = p_i + \mathbf{a}\nabla p_i$. Hence, the bond percolation factor $K_{ij} = p_i p_j$ in the continuum limit becomes

$$K(\mathbf{r}) = p(\mathbf{r})[p(\mathbf{r}) + \mathbf{a}\,\nabla\, p(\mathbf{r})] = p(\mathbf{r}) + \frac{1}{2}\mathbf{a}\,\nabla\, p(\mathbf{r}),$$

leading to

$$K = K(z) = \frac{1}{Na^2}\int d^2\mathbf{r}\left[p(\mathbf{r}) + \frac{1}{2}\mathbf{a}\,\nabla\, p(\mathbf{r})\right]$$
$$= 1 - z + \frac{\mathbf{a}}{2\text{Na}^2}\int d^2\mathbf{r}\,\nabla\, p(\mathbf{r})$$
$$= 1 - z + \frac{\mathbf{a}}{2Na^2}(-1)\sum_{\text{Zn}}\int \text{contours}$$
$$= 1 - z - \frac{\mathbf{a}N_{\text{Zn}}4\mathbf{a}}{2Na^2} = 1 - 3z \tag{A2}$$

Using Stoke's theorem in the above formula we obtained the integration over a contour of the 2D volume, which splits into the sum of contours over Zn impurities. The minus sign accounts for the opposite orientation of the small contours with respect to the larger one.

APPENDIX B: NONLINEAR SIGMA MODEL WITH DILUTION

In La_2CuO_4 the DM vectors are in good approximation perpendicular to the Cu-Cu bonds and change sign from one bond to another, while the *XY* matrices provide an easy-plane anisotropy. It is worth noting that the pure 2D system defined by the action (1) does not display a rotational symmetry, so it can have order at finite temperature without violating the Mermin-Wagner theorem.

Before we proceed with the derivation of the NLSM, let us recall some technical details: $\mathbf{d}_+$ is a vector in the *a* orthorhombic direction; and *i* is an index on a 2D lattice, so *i* should be understood as (p,q) and $(-1)^i$ as $(-1)^{p+q}$. Furthermore, we shall use that

$$\sum_{\langle i,j\rangle} \mathbf{D}_{ij} = \sum_i \mathbf{D}_{i,x} + \mathbf{D}_{i,y} = 2\sum_i \mathbf{d}_{+,i}, \tag{B1}$$

$$\mathbf{\Omega}_i = (-1)^i \mathbf{n}_i + a\mathbf{l}_i - \tfrac{1}{2}(-1)^i a^2 \mathbf{n}_i \mathbf{l}_i^2, \tag{B2}$$

with $\mathbf{n}_i \cdot \mathbf{l}_i = 0$,

$$\mathbf{n}_j = \mathbf{n}_i - r_{ij}^l \partial_l \mathbf{n}_i + \frac{1}{2} r_{ij}^l r_{ij}^m \partial_l \partial_m \mathbf{n}_i, \tag{B3}$$

and finally

$$a^2 \sum_i = \int d^2\mathbf{r}. \tag{B4}$$

Let us first transform the Heisenberg term of the Hamiltonian. Using Eqs. (B2) and (B3) and neglecting $O(a^3)$ terms we get

$$H_H = JS^2 \sum_{\langle i,j\rangle} \mathbf{\Omega}_i \mathbf{\Omega}_j = JS^2 \sum_{\langle i,j\rangle} \left(\frac{1}{2} r_{ij}^l r_{ij}^m \partial_l \mathbf{n}_i \partial_m \mathbf{n}_i + 2a^2 \mathbf{l}_i^2 \right)$$
$$= JS^2 a^2 \sum_i \left(\frac{1}{2} (\nabla \mathbf{n}_i)^2 + 4\mathbf{l}_i^2 \right). \tag{B5}$$

In the continuum limit the Heisenberg Hamiltonian reads

$$H_H = \frac{JS^2}{2} \int d^2\mathbf{r} [(\nabla \mathbf{n})^2 + 8\mathbf{l}^2]. \tag{B6}$$

In the diluted case, we should multiply $\mathbf{\Omega}_i$ with p_i. Hence, Eq. (B5) would be modified as follows:

$$H_H^d = JS^2 \sum_{\langle i,j\rangle} p_i p_j \mathbf{\Omega}_i \mathbf{\Omega}_j,$$

where the index "*d*" stands for "diluted." We want to treat the *static impurities* as an *average effect*, thus we substitute $p_i p_j$ in the above equation with $\langle p_i p_j \rangle = K(\mathbf{r})$, the bond percolation factor (for more details, see Chap. 3 of Ref. 25). We simplify the problem even more by considering the averaged one, taking $\langle K(\mathbf{r}) \rangle = K(z)$ [for the shortening of the notations in what follows we will use *K* instead of $K(z)$], where *z* is the Zn concentration. Thus, in the diluted case Eq. (B6) reads

$$H_H^d = \frac{JS^2 K}{2} \int d^2\mathbf{r} [(\nabla \mathbf{n})^2 + 8\mathbf{l}^2]. \tag{B7}$$

Following a similar procedure, we may transform the DM and *XY* terms of the Hamiltonian. For the DM Hamiltonian we get

$$H_{\mathrm{DM}}^d = \frac{4S^2 K}{a} \int d^2\mathbf{r} [\mathbf{d}_+ \cdot (\mathbf{n} \times \mathbf{l})]. \tag{B8}$$

For the *XY* Hamiltonian in the continuum limit we find

$$H_{XY}^d = \frac{2S^2 K}{a^2} \int d^2\mathbf{r} [(\Gamma_1 - \Gamma_3) n_z^2], \tag{B9}$$

where we neglected the small terms like $\Gamma(\nabla \mathbf{n})^2$ and $\Gamma \mathbf{l}^2$.

Now, we will discuss in detail a Wess-Zumino term in 2D for the diluted case, since it did not appear in the literature. For the 1D case we refer the reader to Ref. 35 (clean system) and Ref. 25 (diluted system).

Following Fradkin (see Appendix A or Ref. 35), we write the Wess-Zumino action on a lattice [notice that (p,q) are the indices along *x* and *y* directions respectively, in contrast with *i* and *j*, which take values on a 2D lattice]

$$\delta S_{\mathrm{WZ}} = \delta \mathbf{\Omega} \cdot \mathbf{\Omega} \times \partial_0 \mathbf{\Omega}, \tag{B10}$$

$$S_{\mathrm{WZ}} = S \int_0^T dx_0 \sum_{p,q} S_{\mathrm{WZ}}[\mathbf{\Omega}(p,q)]$$
$$= \frac{S}{2} \int_0^T \left(\sum_{p=1}^{N_x/2} \sum_{q=1}^{N_y} \{S[\mathbf{\Omega}(2p,q)] + S[\mathbf{\Omega}(2p-1,q)]\} \right.$$
$$\left. + \sum_{p=1}^{N_x} \sum_{q=1}^{N_y/2} \{S[\mathbf{\Omega}(p,2q)] + S[\mathbf{\Omega}(p,2q-1)]\} \right). \tag{B11}$$

In the second and third lines of Eq. (B11) we recognize δS_{WZ}, which can be expressed through $\mathbf{\Omega}$. Using the spin decomposition (B2), we get

$$\delta_x \mathbf{\Omega}(p,q) = \mathbf{\Omega}(2p,q) + \mathbf{\Omega}(2p-1,q)$$
$$= (-1)^{2p} [\mathbf{n}(2p,q) - \mathbf{n}(2p-1,q)]$$
$$+ 2a\mathbf{l}(2p,q) + O(a^2) = a\partial_x \mathbf{n} + 2a\mathbf{l}. \tag{B12}$$

Analogously, we transform the third line of Eq. (B11),

$$\delta_y \mathbf{\Omega}(p,q) = a\partial_y \mathbf{n} + 2a\mathbf{l}. \tag{B13}$$

Let us note that

$$\sum_{p=1}^{N_x/2} \sum_{q=1}^{N_y} = \frac{1}{2} \sum_{\text{all sites}} = \frac{1}{2} \sum_i \to \frac{1}{2a^2} \int d^2\mathbf{r}. \tag{B14}$$

Setting (B10), (B12), and (B13) into (B11) and having in mind (B14), we obtain for the Wess-Zumino action [decomposing (B10) into staggered and uniform components, we keep only first order terms in *a*]

$$S_{\mathrm{WZ}} = \frac{Sa}{4}\int_0^T dx_0 \sum_i [(\nabla \mathbf{n}_i + 4\mathbf{l}_i)\cdot(\mathbf{n}_i \times \partial_0 \mathbf{n}_i)]. \quad \text{(B15)}$$

The first term in Eq. (B15) is a topological term. It was demonstrated by Haldane[36] that in $D>1$ this term sums to zero in the AF background.

The total Euclidean action reads

$$S_E = -iS_{\mathrm{WZ}} + S_H + S_{\mathrm{DM}} + S_{XY}. \quad \text{(B16)}$$

Now we are ready to write a Wess-Zumino Lagrangian,

$$L_{\mathrm{WZ}} = -i\frac{S}{a}\int d^2\mathbf{r}[\mathbf{l}\cdot\mathbf{n}\times\partial_\tau\mathbf{n}]. \quad \text{(B17)}$$

In the presence of *dilution* the action (B17) will be multiplied with P_∞. The explanation is the following: in the expression for δS_{WZ} (B10) we will have a factor p^3, which by definition is equal to p (and we further simplify the problem by taking $\langle p\rangle = P_\infty$). We can carefully do the procedure in Eq. (B11) in the diluted case, but since we neglect $O(a^2)$ terms, the answer will be the same.

Let us now summarize the results obtained so far. The total Euclidean action in the diluted system reads

$$S = \int d\tau L_{\mathrm{tot}}, \quad \text{(B18)}$$

with $L_{\mathrm{tot}} = L_{\mathrm{WZ}} + L_H + L_{\mathrm{DM}} + L_{XY}$ and

$$L_{\mathrm{WZ}} = \frac{-iSP_\infty}{a}\int d^2\mathbf{r}[\mathbf{l}\cdot(\mathbf{n}\times\partial_\tau\mathbf{n})],$$

$$L_H = \frac{JS^2K}{2}\int d^2\mathbf{r}[(\nabla\mathbf{n})^2 + 8\mathbf{l}^2],$$

$$L_{\mathrm{DM}} = \frac{4S^2K}{a}\int d^2\mathbf{r}[\mathbf{d}_+\cdot(\mathbf{n}\times\mathbf{l})],$$

$$L_{XY} = \frac{2S^2K}{a^2}\int d^2\mathbf{r}[(\Gamma_1-\Gamma_3)n_z^2]. \quad \text{(B19)}$$

Now we integrate out $\mathbf{l}$ in a sense of a saddle-point solution. We must find a solution of an equation

$$\frac{\delta L_{\mathrm{tot}}}{\delta \mathbf{l}} = 0$$

and plug it into Eq. (B18). Doing this, we get

$$\mathbf{l} = \frac{iP_\infty}{8JSaK}(\mathbf{n}\times\partial_\tau\mathbf{n}) + \frac{1}{2Ja}(\mathbf{n}\times\mathbf{d}_+) \quad \text{(B20)}$$

and

$$S = \frac{1}{2gc}\int d\tau\int d^2\mathbf{r}\left(\frac{P_\infty}{K}(\partial_\tau\mathbf{n})^2 + Kc^2(\nabla\mathbf{n})^2 + K\mathbf{D}_+^2 n_a^2 + K\Gamma_c n_c^2\right), \quad \text{(B21)}$$

where we defined

$gc = 8Ja^2$ (bare) inverse transverse susceptibility,

$c = 2\sqrt{2}JSa$ (bare) spin-wave velocity,

$\mathbf{D}_+ = \sqrt{2gcS^2/Ja^2}\mathbf{d}_+ = 2\sqrt{2}Sd\vec{e}_a$ DM vector,

$\Gamma_c = (4gcS^2/a^2)(\Gamma_1-\Gamma_3)$ XY anisotropy.

It is convenient to introduce the notations $D_+ = m_a$ and $\Gamma_c = m_c^2$. Setting this into Eq. (B21) and rewriting it in a conventional way we get a final expression for the total action in the presence of dilution,

$$S = \frac{1}{2gcK/P_\infty}\int d\tau\int d^2\mathbf{r}\{(\partial_\tau\mathbf{n})^2 + Z[c^2(\nabla\mathbf{n})^2 + m_a^2 n_a^2 + m_c^2 n_c^2]\}, \quad \text{(B22)}$$

where

$$Z = \frac{K^2}{P_\infty}. \quad \text{(B23)}$$

[1] M. A. Kastner, R. J. Birgeneau, G. Shirane, and Y. Endoh, Rev. Mod. Phys. **70**, 897 (1998).

[2] O. P. Vajk, P. K. Mang, M. Greven, P. M. Gehring, and J. W. Lynn, Science **295**, 1691 (2002).

[3] M. Hücker, V. Kataev, J. Pommer, J. Harass, A. Hosni, C. Pflitsch, R. Gross, and B. Büchner, Phys. Rev. B **59**, R725 (1999).

[4] I. Ya. Korenblit, Amnon Aharony, and O. Entin-Wohlman, Phys. Rev. B **60**, R15017 (1999).

[5] I. Ya. Korenblit, A. Aharony, and O. Entin-Wohlman, Phys. Rev. B **73**, 106501 (2006); M. Hücker, H. H. Klauss, and B. Büchner, *ibid.* **70**, 220507(R) (2004).

[6] V. Juricic, M. B. Silva Neto, and C. Morais Smith, Phys. Rev. Lett. **96**, 077004 (2006).

[7] A. Lüscher, A. I. Milstein, and O. P. Sushkov, Phys. Rev. Lett. **98**, 037001 (2007).

[8] A. N. Lavrov, Y. Ando, S. Komiya, and I. Tsukada, Phys. Rev. Lett. **87**, 017007 (2001).

[9] M. B. Silva Neto, L. Benfatto, V. Juricic, and C. Morais Smith, Phys. Rev. B **73**, 045132 (2006).

[10] A. Gozar, B. S. Dennis, G. Blumberg, Seiki Komiya, and Yoichi Ando, Phys. Rev. Lett. **93**, 027001 (2004).

[11] M. B. Silva Neto and L. Benfatto, Phys. Rev. B **72**, 140401(R) (2005).
[12] Boris I. Shraiman and Eric D. Siggia, Phys. Rev. Lett. **61**, 467 (1988).
[13] F. C. Zhang and T. M. Rice, Phys. Rev. B **37**, R3759 (1988).
[14] C. R. Rotundu, P. Kumar, and B. Andraka, Phys. Rev. B **73**, 014515 (2006).
[15] M. Reehuis, C. Ulrich, K. Prokeš, A. Gozar, G. Blumberg, Seiki Komiya, Yoichi Ando, P. Pattison, and B. Keimer, Phys. Rev. B **73**, 144513 (2006).
[16] J. Chovan and N. Papanicolaou, Eur. Phys. J. B **17**, 581 (2000).
[17] K. V. Tabunshchyk and R. J. Gooding, Phys. Rev. B **71**, 214418 (2005).
[18] A. Lüscher, G. Misguich, A. I. Milstein, and O. P. Sushkov, Phys. Rev. B **73**, 085122 (2006).
[19] S. Chakravarty, B. I. Halperin, and D. R. Nelson, Phys. Rev. B **39**, 2344 (1989).
[20] L. Shekhtman, O. Entin-Wohlman, and A. Aharony, Phys. Rev. Lett. **69**, 836 (1992).
[21] W. Koshibae, Y. Ohta, and S. Maekawa, Phys. Rev. B **50**, 3767 (1994).
[22] Yu-Chang Chen and A. H. Castro Neto, Phys. Rev. B **61**, R3772 (2000).
[23] V. Y. Irkhin, A. A. Katanin, and M. I. Katsnelson, Phys. Rev. B **60**, 1082 (1999).
[24] V. Y. Irkhin and A. A. Katanin, Phys. Rev. B **60**, 2990 (1999).
[25] The derivation of the dependence on doping of site and bond percolation factor can be found in Appendix C of this thesis: Yu-Chang Chen, Ph.D. thesis, http://yuchang.info/images/dist.pdf
[26] A. Brooks Harris and Scott Kirkpatrick, Phys. Rev. B **16**, 542 (1977).
[27] B. P. Watson and P. L. Leath, Phys. Rev. B **9**, 4893 (1974).
[28] A. W. Sandvik, Phys. Rev. B **66**, 024418 (2002); Phys. Rev. Lett. **89**, 177201 (2002).
[29] S. Sachdev, Phys. Rev. B **49**, 6770 (1994).
[30] L. Benfatto and M. B. Silva Neto, Phys. Rev. B **74**, 024415 (2006); L. Benfatto, M. B. Silva Neto, A. Gozar, B. S. Dennis, G. Blumberg, L. L. Miller, S. Komiya, and Y. Ando, *ibid.* **74**, 024416 (2006).
[31] M. Matsuda, M. Fujita, K. Yamada, R. J. Birgeneau, M. A. Kastner, H. Hiraka, Y. Endoh, S. Wakimoto, and G. Shirane, Phys. Rev. B **62**, 9148 (2000).
[32] N. Hasselmann, A. H. Castro Neto, and C. Morais Smith, Phys. Rev. B **69**, 014424 (2004).
[33] M. Matsuda, M. Fujita, and K. Yamada, Phys. Rev. B **73**, 140503(R) (2006).
[34] T. Thio, T. R. Thurston, N. W. Preyer, P. J. Picone, M. A. Kastner, H. P. Jenssen, D. R. Gabbe, C. Y. Chen, R. J. Birgeneau, and A. Aharony, Phys. Rev. B **38**, 905(R) (1988); T. Thio and A. Aharony, Phys. Rev. Lett. **73**, 894 (1994).
[35] E. Fradkin and M. Stone, Phys. Rev. B **38**, 7215 (1988).
[36] F. D. M. Haldane, Phys. Rev. Lett. **61**, 1029 (1988).